Atmos. Chem. Phys. Discuss., https://doi.org/10.5194/acp-2019-271
Manuscript under review for journal Atmos. Chem. Phys.
Discussion started: 8 April 2019

Atmospheric Chemistry and Physics Discussions

Chamber-based insights into the factors controlling IEPOX SOA yield, composition, and volatility

Emma L. D'Ambro[1,2], Siegfried Schobesberger[1,3], Cassandra J. Gaston[1,a], Felipe D. Lopez-Hilfiker[1,b], Ben H. Lee[1], Jiumeng Liu[4,c], Alla Zelenyuk[5], David Bell[5,d], Christopher D. Cappa[6,7], Taylor Helgestad[6,e], Ziyue Li[7], Alex Guenther[5,f], Jian Wang[8,g], Matthew Wise[9], Ryan Caylor[9], Jason D. Surratt[10], Theran Riedel[10], Noora Hyttinen[11,h], Vili-Taneli Salo[11], Galib Hasan[11], Theo Kurtén[11], John E. Shilling[4], Joel A. Thornton[1,2]

[1]Department of Atmospheric Sciences, University of Washington, Seattle WA, USA
[2]Department of Chemistry, University of Washington, Seattle WA, USA
[3]Department of Applied Physics, University of Eastern Finland, Kuopio, Finland
[4]Atmospheric Sciences and Global Change Division, Pacific Northwest National Laboratory, Richland WA, USA
[5]Environmental Molecular Sciences Laboratory, Pacific Northwest National Laboratory, Richland WA, USA
[6]Department of Civil and Environmental Engineering, University of California, Davis CA, USA
[7]Atmospheric Science Graduate Group, University of California, Davis CA, USA
[8]Environmental and Climate Sciences Department, Brookhaven National Laboratory, Upton NY, USA
[9]Department of Math and Science, Concordia University, Portland OR, USA
[10]Department of Environmental Sciences and Engineering, Gillings School of Global and Public Health, University of North Carolina, Chapel Hill NC, USA
[11]Department of Chemistry and Institute for Atmospheric and Earth System Research (INAR), University of Helsinki, Helsinki, Finland
[a]now at: Rosenstiel School of Marine & Atmospheric Science, University of Miami FL, USA
[b]now at: TofWerk AG, Thun, Switzerland
[c]now at: School of Environment, Harbin Institute of Technology, Harbin, Heilongjiang, China
[d]now at: Laboratory of Atmospheric Chemistry, Paul Scherrer Institute, PSI-Villigen, Switzerland
[e]now at: California Air Resources Board, Sacramento CA, USA
[f]now at: Department of Earth System Science, University of California, Irvine, USA
[g]now at: Center for Aerosol Science and Engineering, Department of Energy, Environmental and Chemical Engineering, Washington University in St. Louis, St. Louis MO, USA
[h]now at: Nano and Molecular Systems Research Unit, University of Oulu, Oulu, Finland

Atmos. Chem. Phys. Discuss., https://doi.org/10.5194/acp-2019-271
Manuscript under review for journal Atmos. Chem. Phys.
Discussion started: 8 April 2019

Atmospheric Chemistry and Physics Discussions

Abstract

We present measurements utilizing the Filter Inlet for Gases and Aerosols (FIGAERO) applied to chamber measurements of isoprene-derived epoxydiol (IEPOX) reactive uptake to aqueous acidic particles and associated SOA formation. Similar to recent field observations with the same instrument, we detect two molecular components desorbing from the IEPOX SOA in high abundance: $C_5H_{12}O_4$ and $C_5H_{10}O_3$. The thermal desorption signal of the former, presumably 2-methyltetrols, exhibits two distinct maxima, suggesting it arises from at least two different SOA components with significantly different effective volatilities. Isothermal evaporation experiments illustrate that the most abundant component giving rise to $C_5H_{12}O_4$ is semi-volatile, undergoing nearly complete evaporation within 1 hour, while the second, less volatile, component remains unperturbed and even increases in abundance. We thus confirm, using controlled laboratory studies, recent analyses of ambient SOA measurements showing that IEPOX SOA is of very low volatility and commonly measured IEPOX SOA tracers, such as 2-methyltetrols and C_5-alkene triols, result predominantly from artifacts of measurement techniques associated with thermal decomposition and/or hydrolysis. We further show that IEPOX SOA volatility continues to evolve via acidity enhanced accretion chemistry on the timescale of hours, potentially involving both 2-methyltetrols and organosulfates.

Introduction

Aerosols less than 1 μm in diameter play particularly important roles in the Earth's radiative balance and air quality, a large fraction of which is organic carbonaceous material of biogenic origin (~70%) (Hallquist et al., 2009). Isoprene, with a global emission rate of 500 TgC $year^{-1}$ (Guenther et al., 2012), has the potential to form significant quantities of secondary organic aerosol (SOA). The ability of a volatile organic compound (VOC) to form SOA depends on either of two factors: the efficiency of its oxidative conversion to lower volatility products that can partition to the condensed phase, or the reaction of gas-phase oxidation products in the condensed phase to form products which remain in the condensed phase. Each of these two SOA formation mechanisms have been heavily studied in the case of isoprene.

The atmospheric oxidation of isoprene under low NO conditions typically proceeds by OH radicals, leading to the formation of first generation isoprene hydroxy hydroperoxides (ISOPOOH) in high yield (70%) (Paulot et al., 2009). The remaining double bond of isoprene can then undergo another OH addition, leaving a carbon-centered radical adjacent to a hydroperoxide moiety. This radical can internally rearrange to form an epoxy diol (IEPOX) at a yield of ~70-80% (St Clair et al., 2016) or undergo addition of O_2 to form a peroxy radical. The peroxy radical undergoes bimolecular reactions to form closed shell hydroperoxide or nitrate products, or unimolecular H-shifts to form carbonyl- and epoxide-containing products (D'Ambro et al., 2017b; Paulot et al., 2009). The bimolecular peroxy radical reaction products have been shown to be of sufficiently low volatility to partition to the aerosol-phase (D'Ambro et al., 2017a; Liu et al., 2016), and IEPOX has been shown to react in aqueous acidic particles, forming SOA. Commonly measured species from IEPOX reactive uptake include 2-methyltetrols (Lin et al., 2012; Surratt et al., 2006; Surratt et al., 2010; Wang et al., 2005), C_5-alkene triols (Lin et al., 2012; Surratt et al., 2006; Surratt et al., 2010; Wang et al., 2005), organosulfates (Lin et al., 2012; Surratt et al., 2007a; Surratt et al., 2007b; Surratt et al., 2010), 3-methyltetrahydrofuran-3,4-diols (3-MeTHF-3,4-diols) (Lin et al., 2012), and oligomers (Lin et al., 2012; Lin et al., 2014; Surratt et al., 2010).

Atmos. Chem. Phys. Discuss., https://doi.org/10.5194/acp-2019-271
Manuscript under review for journal Atmos. Chem. Phys.
Discussion started: 8 April 2019

Atmospheric Chemistry and Physics Discussions

Recently, studies have called into question whether these commonly measured monomeric products of IEPOX multiphase chemistry exist in the particle-phase as measured. We showed previously that components of organic aerosol in the Southeast U.S. with compositions of $C_5H_{10}O_3$ and $C_5H_{12}O_4$ desorbed at much higher temperatures, and therefore much lower volatilities, than would be expected based on their composition (Lopez-Hilfiker et al., 2016). We concluded that the measured compositions arise from lower volatility material in the SOA that thermally decomposes rather than evaporating as the native species, and that, based on the relative abundance of these lower volatility components, IEPOX SOA as a whole is typically comprised of very low volatility material. When IEPOX was reacted in bulk solutions and analyzed via nuclear magnetic resonance, no evidence was found for the production of C_5-alkene triols or 3-MeTHF-3,4-diols, and although a second isomer of the MeTHF diol was observed (3-MeTHF-2,4-diols), the formation rate from IEPOX was calculated to be so slow relative to nucleophilic addition that its formation would be limited to situations where the aerosol had low water content (Watanabe et al., 2018). These findings were further corroborated by comparing a novel chromatography technique that does not involve heating to traditional GC/EI-MS analysis of IEPOX SOA compositions, finding that alkene triols and 3-MeTHF-3,4-diols were in fact formed via thermal decomposition of 2-methyltetrol sulfates and 3-methyltetrol sulfates, respectively (Cui et al., 2018).

An additional challenge to understanding IEPOX SOA is that there remains a large gap in carbon closure resulting from IEPOX reactive uptake to aqueous acidic aerosol particles. Although the reactivity of IEPOX in acidic particles is high (Gaston et al., 2014), the SOA yield per reactive loss of IEPOX to particles is relatively low and varies greatly depending on aerosol composition, from approximately 3 to 21% (Riedel et al., 2015). This disconnect may present an inconsistency in models that simulate both IEPOX and IEPOX-derived SOA. If such low yields are indeed realistic, models that adjust the rate of IEPOX reactive uptake to match the IEPOX SOA tracer concentrations without accounting for the lower yield may not correctly simulate IEPOX distributions where reactive uptake is a dominant sink for IEPOX (Gaston et al., 2014).

In this work we seek to understand the nature of products formed via the reactive uptake of IEPOX in aqueous acidic particles and the flow of carbon between the gas- and particle-phases. We present measurements from the Pacific Northwest National Laboratory (PNNL, Richland WA) environmental chamber during the 2015 SOA Formation from Forest Emissions Experiment (SOAFFEE) campaign. Batch and continuous flow mode experiments were performed with authentic *trans*-β-IEPOX, which is the dominant isomer (Bates et al., 2014), and wet acidic seed to study the products of IEPOX uptake and the resulting aerosol properties. The properties of commonly measured IEPOX uptake products, the 2-methyltetrols ($C_5H_{12}O_4$) and C_5-alkene triols or 3-MeTHF-3,4-diols ($C_5H_{10}O_3$), such as volatility and solubility, are examined in the context of experiments utilizing isothermal evaporation of the formed SOA. The effect of acidity versus liquid water content on the products formed is also discussed, along with implications for modeling atmospheric IEPOX and its conversion into SOA.

Experimental Methods

Experiments were performed at the Pacific Northwest National Laboratory (PNNL) as part of the Secondary Organic Aerosol Formation from Forest Emissions Experiments (SOAFFEE) campaign held during the summer of 2015. PNNL's 10.6 m^3 fluorinated ethylene propylene (FEP) environmental chamber has been described in detailed previously (Liu et al., 2012). The chamber was run in both batch mode and continuous flow mode. In batch mode the

experiments lasted ~10 hours, while in continuous flow mode the total flow rate was 48.2 L min^{-1} resulting in a residence time of ~3.7 hours.

Aliquots of an authentic *trans*-β-IEPOX standard, synthesized according to Zhang et al. (2012), dissolved in ethyl acetate were injected into a glass bulb which was connected to the chamber via ~10 cm of ¼" OD polytetrafluoroethylene (PTFE) tubing to achieve 2 ppb in steady state and at the beginning of batch modes. The bulb and transfer line were heated to 30-40 ºC and a 100-300 sccm flow of zero air passed over the IEPOX to vaporize and carry it into the chamber. Typically, we measured ~ 10 µg m^{-3} of IEPOX prior to aqueous seed addition. Given calibration uncertainties of ~ +/- 30% from repetitive injections and analytical errors, and potential losses on chamber and sampling surfaces, we estimate an uncertainty of approximately +/- 50% for gas phase IEPOX concentrations and other tracers. An ammonium bisulfate solution acidified with additional H_2SO_4 was atomized to generate wet, polydisperse acidic ammonium sulfate seed which were added to the chamber at concentrations sufficiently large that condensation of IEPOX onto the particles was competitive with the chamber walls. Continuous flow experiments were conducted at 50% RH, while the RH of batch mode experiments was either 30% or 50%. The seed surface area concentration was 6.0 ± 0.3 $\times 10^8$ nm^2 cm^{-3} for all experiments. The average NH_4^+ concentrations measured by the AMS were 1.1, 2.4, and 2.7 µg m^{-3} at steady state, 30% RH batch, and 50% RH batch, respectively. The average SO_4^{2-} concentrations were 4.1, 13.0, and 10.4 µg m^{-3} at steady state, 30% RH batch, and 50% RH batch, respectively. The NH_4^+/SO_4^{2-} mole ratio of chamber aerosol as measured by the AMS during these experiments was typically between 0.7 and 1.5, implying some excess NH_3 present in the chamber was partitioning to the seed, but that the aerosol remained acidic prior to injection of IEPOX. The corresponding aerosol pH range determined from the E-AIM aerosol thermodynamics model was 0.3 to 1 (Wexler and Clegg, 2002).

A suite of online gas and particle-phase instrumentation was used to monitor concentrations throughout the experiments. Aerosol number and volume concentrations were measured with a scanning mobility particle sizer (SMPS, TSI model 3936), O_3 and $NO/NO_2/NO_x$ concentrations were monitored with commercial instrumentation (Thermo Environmental Instruments models 49C and 42C, respectively). An Aerodyne high-resolution time-of-flight mass spectrometer (HRToF-AMS) was utilized to measure bulk submicron organic and inorganic aerosol composition.

A high-resolution time-of-flight chemical ionization mass spectrometer (HRToF-CIMS) using iodide adduct ionization was deployed for the detection of both semi- and low-volatility organic compounds (Lee et al., 2014). The HRToF-CIMS was used to monitor the evolving concentrations of both the precursor (IEPOX) and reaction products in both the gas- and particle-phases when coupled to a Filter Inlet for Gases and AEROsols (FIGAERO), from here on referred to as FIGAERO-CIMS. The coupling, optimization, and operation of this combination has been described in detail previously (Lopez-Hilfiker et al., 2014) and is nearly identical to previous operations (D'Ambro et al., 2017a; D'Ambro et al., 2017b). Briefly, the FIGAERO is an inlet manifold that allows for semi-continuous measurements of both gases and aerosols with approximately hourly resolution. Aerosol was collected on a 24 mm PTFE filter for 43 minutes at 2.5 L min^{-1}, during which the gases were measured in real time. Following collection, programmatically heated ultra-high purity (UHP) N_2 was passed over the filter, while the

Atmos. Chem. Phys. Discuss., https://doi.org/10.5194/acp-2019-271
Manuscript under review for journal Atmos. Chem. Phys.
Discussion started: 8 April 2019

temperature was ramped from ambient to 200 ºC at a rate of 10 ºC min^{-1} in order to thermally desorb compounds from the particle-phase to the gas-phase to be carried into the CIMS for detection. After the temperature was ramped, it was held at 200 ºC for 50 minutes to allow species to desorb and signals to return to background levels. Particle blanks were conducted approximately every fourth desorption during continuous flow mode or at the beginning and end of each batch mode experiment by inserting a secondary filter upstream of the primary FIGAERO filter in order to get a measure of the gas adsorption artifact on the primary filter. Gas zeros were conducted every 2 minutes by over blowing the CIMS pinhole flow with UHP N_2. The specific coupling to a HRToF-CIMS with iodide ions allows detailed molecular analysis of hundreds of oxygenated organic compounds via a clustering, fragmentation-free ionization process.

The FIGAERO-CIMS was also utilized to perform isothermal evaporation experiments as have been described previously (D'Ambro et al., 2018). In normal operation, the programmatic thermal desorption is begun immediately after moving the FIGAERO filter under the heating tube. During isothermal evaporation experiments however, the aerosol is instead exposed for one hour to a stream of ambient temperature UHP N_2 humidified to 50% RH by using a water bubbler and two mass flow controllers (Figure 1). After the hour exposure, the N_2 flow is reverted to its normal dry state and the programmatic heating proceeds as normal. See Figure 1 for the experimental setup. The RH of 50% during evaporation periods was chosen to match that of the chamber to keep the phase state of the collected aerosols the same (i.e. so as to not drive efflorescence). Only the isothermal evaporation portion of the experiment was humidified; during the thermal desorption the bubbler was isolated using two solenoid valves. Passing excess humidified N_2 over the aerosol and into the instrument resulted in a constant dilution of the vapor-phase, which allowed for any semi-volatile material to evaporate and also be carried into the CIMS for detection.

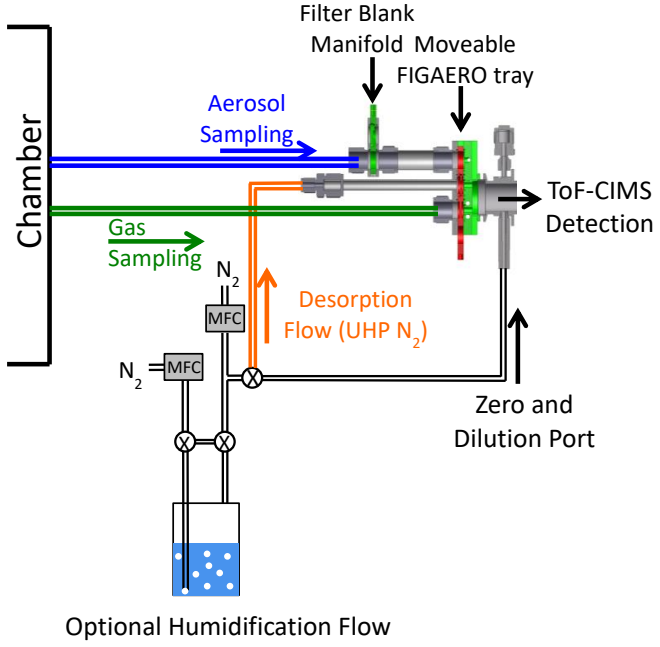

Figure 1. Schematic of the FIGAERO isothermal evaporation setup.

Atmos. Chem. Phys. Discuss., https://doi.org/10.5194/acp-2019-271
Manuscript under review for journal Atmos. Chem. Phys.
Discussion started: 8 April 2019

Atmospheric Chemistry and Physics Discussions

Results & Discussion

Chamber-generated IEPOX SOA Composition and Volatility

Our primary goals with this experiment were to assess whether chamber-generated IEPOX SOA had a composition and volatility similar to that inferred from field measurements using the FIGAERO-CIMS of various IEPOX tracers and to test whether IEPOX SOA as a whole or some of its components were semi-volatile as expected from mechanistic and kinetic considerations. Overall, the estimated mass yield of OA from IEPOX exposure to aqueous acidic seed was generally less than unity, of order 0.5 to less than 0.25, somewhat higher than estimates from Riedel et al [2015]. Mean organic aerosol (OA) mass concentrations generated when IEPOX and aqueous acidic seed were 2.5 μg m^{-3} for steady state conditions, 5.5 μg m^{-3} at the beginning of the 30% RH batch experiment, and 4.5 μg m^{-3} at the beginning of the 50% RH batch experiment. The OA to sulfate ratio was observed to evolve during a batch experiment (e.g., decreasing by 20% from the peak), and given the uncertainties associated with potential vapor wall losses of IEPOX and its reaction products, we refrain from quantitatively interpreting the SOA yield behaviors in detail.

Regardless of the conditions, the uptake of an authentic IEPOX standard onto acidic seeds in these experiments results in a rather simple observed particle-phase composition upon thermal desorption. As shown in Figure 2, a few compositions dominate the average particle-phase mass spectra, most predominantly $C_5H_{12}O_4$ and $C_5H_{10}O_3$. Both of these species have been repeatedly shown to be major components of IEPOX SOA (Lin et al., 2012; Surratt et al., 2006; Surratt et al., 2010; Wang et al., 2005), although the relative abundances could change with time or conditions. In ambient aerosol in the Southeast U.S., the same FIGAERO-CIMS instrument detected $C_5H_{12}O_4$ and $C_5H_{10}O_3$ in SOA, and these tracers correlated with and explained ~50% of the IEPOX SOA mass derived from factor analysis of aerosol mass spectrometer (AMS) data (Lopez-Hilfiker et al., 2016). Our laboratory chamber experiments starting with an authentic IEPOX standard and acidic seed without photochemical oxidants therefore support the use of these FIGAERO-CIMS compositions as tracers of IEPOX SOA in atmospheric particles. As these two compositions are such a large component of the particle-phase signal (97.5%) measured by FIGAERO-CIMS in chamber generated IEPOX SOA, the properties of the corresponding SOA are presumably similar to their properties.

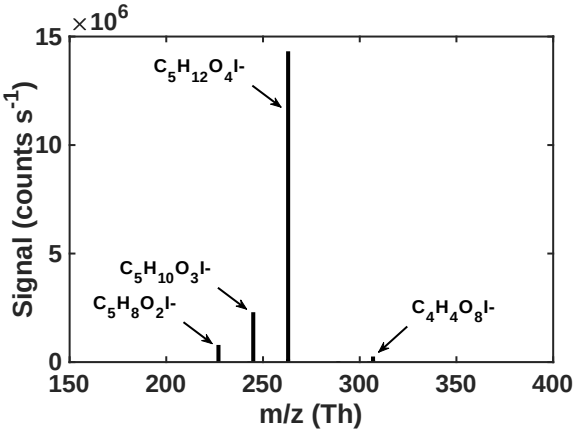

Figure 2. Average mass spectrum of IEPOX-derived SOA at a total OA concentration of 5 μg m^{-3}.

Atmos. Chem. Phys. Discuss., https://doi.org/10.5194/acp-2019-271
Manuscript under review for journal Atmos. Chem. Phys.
Discussion started: 8 April 2019

Atmospheric Chemistry and Physics Discussions

In previous work, we have related the temperature at which the ion signal for a given molecular composition reaches a maximum during a desorption, known as the T_{max}, to the enthalpy of vaporization (or sublimation) and thus effective volatility (Lopez-Hilfiker et al., 2014). Effective volatility refers to the fact that the thermal desorption signal is a convolution of evaporation, thermal decomposition, particle viscosity, and mass transfer of desorbed vapors through the apparatus, and not solely saturation vapor pressure. Notably, the thermogram of $C_5H_{12}O_4$ for chamber generated IEPOX SOA is bimodal (Figure 3, top), i.e. it exhibits two distinct maxima, one occurring at T_{max} = 55 °C (~ 40% of signal), and a second mode at T_{max} = 90 °C. These two maxima indicate SOA components with orders of magnitude different effective volatilities contribute to the desorption of $C_5H_{12}O_4$. For example, using the calibration curve in Lopez-Hilfiker et al. (2014) relating saturation vapor concentration (c*) to T_{max}, the two modes correspond to SOA components with an effective c* of 50 and 0.005 μg m^{-3}. The lower temperature, higher volatility mode of the $C_5H_{12}O_4$ desorption has a T_{max} consistent with that of an authentic 2-methyltetrol standard, synthesized according to Bondy et al. (2018), deposited on the filter (gray dashed line, Figure 3, top). For comparison, if the structure of $C_5H_{12}O_4$ were assumed to be a 2-methyltetrol, group contribution methods predict the c* to be 34 μg m^{-3} (Compernolle et al., 2011), remarkably similar to what the FIGAERO T_{max}-c* relationship predicts for the lower T_{max} mode of the $C_5H_{12}O_4$ thermogram.

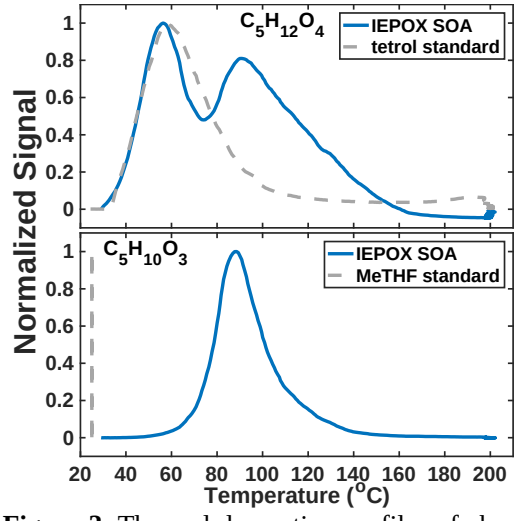

Figure 3. Thermal desorption profiles of chamber aerosol (blue) and calibrations with authentic standards (gray, dashed) of the two major particle-phase compounds detected in the chamber: $C_5H_{12}O_4$ (top) and $C_5H_{10}O_3$ (bottom).

The $C_5H_{10}O_3$ thermogram, in contrast, is monomodal, suggesting a single component giving rise to its desorption. However, the T_{max} is much higher than the corresponding authentic *cis*-3-MeTHF-3,4-diol standard, synthesized according to Zhang et al. (2012), (and also that of an alkane triol standard). This standard desorbs completely from the FIGAERO filter in seconds without heating (gray dashed line, Figure 3, bottom). The T_{max} of $C_5H_{10}O_3$ desorbing from IEPOX SOA is 90 °C, the same as the higher T_{max} mode of the $C_5H_{12}O_4$ component, and thus implies a SOA component with an effective c* of at most 0.005 μg m^{-3}, indicative of thermal decomposition during desorption. For comparison, if the structure is assumed to be a C_5-alkene

triol or 3-MeTHF-3,4-diol, group contribution methods would predict a much larger c* of ~60 or 1.3×10^5 µg m^{-3}, respectively (Compernolle et al., 2011). For comparison, the group contribution predicted c* of *trans*-β-IEPOX is 1.7×10^4 µg m^{-3}. All of this evidence indicates that $C_5H_{10}O_3$, as detected in the chamber-generated SOA, is a result of thermal decomposition of a lower volatility species, consistent with recent studies that found the C_5-alkene triol was not present as a product of bulk IEPOX reactions (Watanabe et al., 2018) or when the IEPOX SOA was analyzed with novel methods not involving heating (Cui et al., 2018). Taken together, the thermograms of $C_5H_{12}O_4$ and $C_5H_{10}O_3$ therefore indicate a large fraction of the chamber generated IEPOX SOA is composed of very low volatility material (effective c* << 1 µg m^{-3}) and several orders of magnitude lower volatility than the compounds that are detected upon thermal desorption.

The thermogram behaviors of chamber generated IEPOX SOA are entirely consistent with those observed for the same tracers measured in ambient aerosol in the Southeast U.S., where $C_5H_{12}O_4$ was also detected with two modes in the thermogram, the respective areas of which varied relative to each other over the course of the measurement campaign (Lopez-Hilfiker et al., 2016). Lopez-Hilfiker et al. (2016) demonstrated from these field observations that the abundance and variability of the lower T_{max} (semi-volatile) mode was consistent with an organic compound having the measured molecular composition and c* of the 2-methyltetrol undergoing equilibrium gas-particle partitioning, while the higher T_{max} mode and that of the $C_5H_{10}O_3$ arose from the decomposition of accretion products.

Insights into Volatility via Isothermal Evaporations

The above considerations of chamber generated IEPOX SOA suggest that a large fraction (the high T_{max} mode) should be relatively stable against evaporation upon dilution of the gas-phase, while the lower T_{max} mode of the $C_5H_{12}O_4$ (2-methyltetrol) component should respond to dilution by evaporating from the particle-phase. To test this hypothesis, we conducted isothermal evaporation experiments using IEPOX SOA generated in the chamber.

Figure 4 shows an example ion signal time series during an isothermal evaporation experiment for $C_5H_{12}O_4$. $C_5H_{12}O_4$ is detected in the gas-phase during particle collection (middle panel, blue shaded area) when chamber air containing IEPOX, acidic aqueous sulfate particles, and IEPOX SOA was being continuously sampled by the FIGAERO-CIMS. The gas-phase sampling included scanning of the dilution ratio, which resulted in varying signals, as well as periodic zeros resulting in occasional significant short-duration drops in signal. We show the last 15-minute portion of the cycle in the gas-phase (blue shaded region) when dilution was held constant, but zeros are still visible as the 2 dips in signal. The chamber was at steady state and the changing gas-phase signal is due to conditioning of the IMR and inlet tubing. During the isothermal evaporation period (yellow shaded area), $C_5H_{12}O_4$ is also detected when a continuous flow of humidified UHP N_2 passes over the particles collected from the chamber on the FIGAERO filter and into the mass spectrometer, consistent with $C_5H_{12}O_4$ evaporation from the collected particles at room temperature (i.e. without heating). Finally, during the temperature-programmed thermal desorption, another pulse of $C_5H_{12}O_4$ was detected corresponding to components in the remaining SOA that desorbed at elevated temperature (green shaded area).

Atmos. Chem. Phys. Discuss., https://doi.org/10.5194/acp-2019-271
Manuscript under review for journal Atmos. Chem. Phys.
Discussion started: 8 April 2019

Atmospheric Chemistry and Physics Discussions

The mass concentration of $C_5H_{12}O_4$ measured during a normal temperature-programmed thermal desorption is compared to that measured during the isothermal evaporation and subsequent desorption (Figure 4, bottom). Mass closure is achieved to within the experimental error, driven by variance in normal temperature-programed thermal desorptions due to chamber conditions and the water vapor effect on CIMS sensitivity (Lee et al., 2014). The observed behaviors, namely detectable gas-phase concentrations of $C_5H_{12}O_4$ in the chamber and isothermal evaporation of $C_5H_{12}O_4$ from collected particles indicate that *(i)* $C_5H_{12}O_4$ is produced from IEPOX reactive uptake, as expected given that the 2-methyltetrol is predicted to be a major product (Eddingsaas et al., 2010), and *(ii)* a portion of the detected $C_5H_{12}O_4$ behaves as a semi-volatile organic compound (SVOC), being present in both the gas- and particle-phases, and evaporating promptly from the particle-phase in response to dilution of the surrounding organic vapors at room temperature.

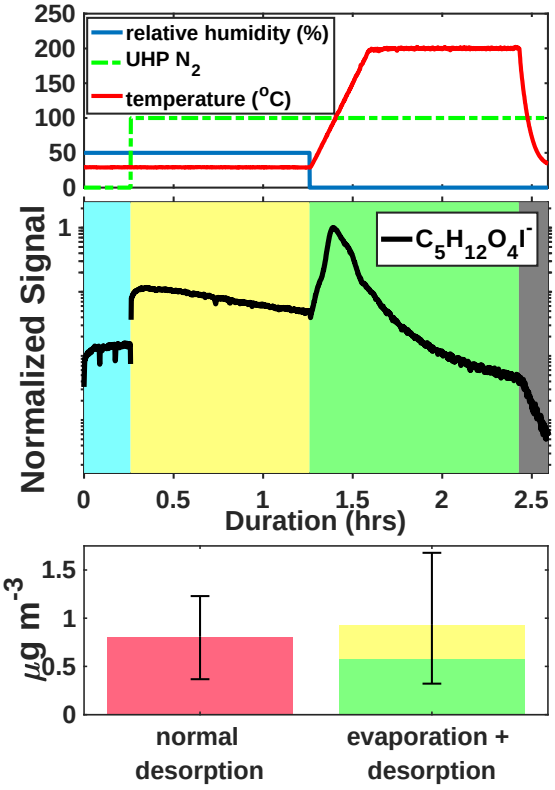

Figure 4. Schematic of the isothermal evaporation process. Top: relative humidity (blue), N_2 flow (green), and temperature (red). Middle: $C_5H_{12}O_4I$- during a 1-hour isothermal evaporation experiment shaded by the phase of the experiments: simultaneous real-time gas-phase sampling and offline aerosol collection (blue), isothermal evaporation where compounds are measured as they evaporate off the filter (yellow), temperature-programmed thermal desorption (green), and cool down of the heating tube (gray). Bottom: mass concentration of $C_5H_{12}O_4$ measured during a normal desorption (pink, left), versus the isothermal evaporation + desorption (yellow and green, right) for the same chamber conditions.

Atmos. Chem. Phys. Discuss., https://doi.org/10.5194/acp-2019-271
Manuscript under review for journal Atmos. Chem. Phys.
Discussion started: 8 April 2019

Atmospheric Chemistry and Physics Discussions

After 1 hour of exposure to UHP N_2 at 50% RH, only 16% of the lower T_{max} mode of the $C_5H_{12}O_4$ thermogram remains, suggesting the free 2-methyltetrol monomer has almost completely evaporated (Figure 5, top). The observed rate of decay (84% hr^{-1}) upon dilution can be related to an effective c*, or, as the 2-methyltetrol is likely to partition into the aqueous-phase, an effective Henry's law constant. Assuming no particle-phase diffusion limitations but accounting for FIGAERO mass transfer limitations (Schobesberger et al., 2018), we predict a c* of 5-15 µg m^{-3} for the portion of the $C_5H_{12}O_4$ thermogram that evaporates. Utilizing COSMOtherm (2018) with the BP_TZVPD_FINE_18 parameterization as described previously (Kurtén et al., 2018), a Henry's law constant of 4.9×10^8 – 1.1×10^{10} M atm^{-1} is predicted if all conformers are used (4.9×10^8 M atm^{-1}) or if the number of internal H-bonds is minimized (1.1×10^{10} M atm^{-1}), which compares well to the value calculated from the observed decay of $C_5H_{12}O_4$ during the evaporation (1.8×10^8 M atm^{-1}). These estimates do not include the likelihood of a salting-out effect expected for the 2-methyltetrol (Waxman et al., 2015), which would further lower the Henry's Law constant. Whether Raoult's or Henry's law is the appropriate framework for interpretation depends on whether IEPOX reactive uptake results in a phase-separated organic medium, for example an organic coating, or a homogeneous aqueous solution, and the competitive partitioning of the 2-methyltetrol between two such regimes. Regardless, as we show below, the semi-volatile nature of the 2-methyltetrol, a major product of IEPOX reactive uptake, will cause it to partition strongly to the gas-phase under typical atmospheric conditions outside of cloud.

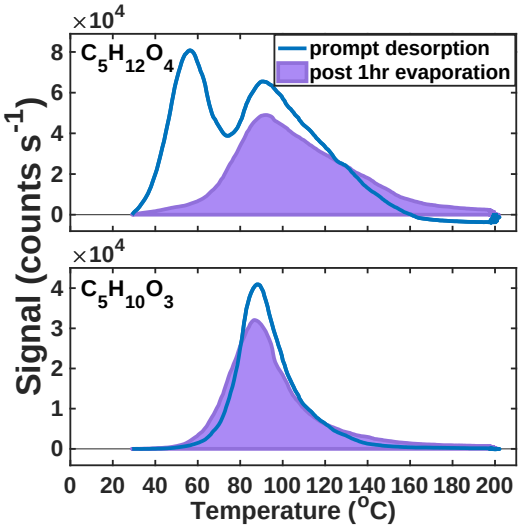

Figure 5. Thermograms obtained from prompt desorption of the aerosol (blue) and after one hour of evaporation (lavender, shaded) of the two major particle-phase compounds detected in the chamber: $C_5H_{12}O_4$ (top) and $C_5H_{10}O_3$ (bottom).

Atmos. Chem. Phys. Discuss., https://doi.org/10.5194/acp-2019-271
Manuscript under review for journal Atmos. Chem. Phys.
Discussion started: 8 April 2019

Atmospheric Chemistry and Physics Discussions

The second, higher T_{max} mode of the $C_5H_{12}O_4$ thermogram and the single Gaussian-like thermogram of $C_5H_{10}O_3$ (Figure 5, bottom) do not change significantly after 1-hour of exposure to UHP N_2. In the case of the $C_5H_{10}O_3$ thermogram, nearly 95% of signal remains after the 1-hour evaporation period. In both cases, there is a slight broadening of the thermogram and a measurable increase in material desorbing at the highest temperatures (120+ ^oC). Previous isothermal evaporation experiments with the FIGAERO have shown that, for α-pinene ozonolysis SOA, the physical age of the aerosol had a controlling role in the volatility of the bulk SOA and individual desorbing compounds (D'Ambro et al., 2018), consistent with the additional hour of non-oxidative aging in this system resulting in an increase in lower-volatility material. As to the widening of the thermograms, Schobesberger et al. (2018) showed that a shallowing of the low temperature side of the thermogram and a broadening of the higher temperature tail correspond to thermal decomposition from a larger suite of bonds with different dissociation energies, consistent with continued formation of a variety of accretion products during the isothermal evaporation period.

The above evidence supports the previous assertions of Lopez-Hilfiker et al. (2016) that the lower T_{max} mode of the $C_5H_{12}O_4$ thermogram corresponds to a semi-volatile component, very likely the 2-methyltetrol, and further support the conclusion that IEPOX SOA in ambient aerosol is very to extremely low volatility. The isothermal evaporation experiments presented above provide an explanation as to why the ambient SOA contained such a relatively small fraction of the low T_{max} (semi-volatile) 2-methyltetrol component in that it likely had evaporated to maintain gas-particle equilibrium. Furthermore, the high T_{max} tracers do not decay in abundance during the evaporation experiments, but rather slightly increase with time at the highest temperatures (>120 ^oC), indicating ongoing accretion chemistry leading to lower volatility components.

Effect of RH and Acidity on IEPOX SOA Characteristics: Mechanistic Insights

We performed two time-dependent "batch mode" chamber experiments using IEPOX and acidic aqueous seed particles, one at 30% and the other at 50% RH. By operating in batch mode as opposed to continuous flow mode, we are able to temporally resolve the formation of SOA. By varying the RH, we simultaneously varied the liquid water content relative to sulfate, and therefore also acidity. Three sequential thermal desorptions of $C_5H_{12}O_4$ obtained over the course of experiments (~10 hrs total) at 30% (left) and 50% (right) RH are shown in Figure 6, top. At 30% RH, the lower T_{max} (higher-volatility) mode grows in rapidly and is clearly visible in the first desorption (black line). The first desorption occurred after 43 minutes of particle collection, which began immediately after the seed was injected into the chamber and IEPOX uptake was initiated, resulting in collected aerosols having a variety of ages and thus the median age of 22 min is assumed. However, this mode then does not grow significantly larger as the experiment progresses. During the 2^{nd} and 3^{rd} desorptions, 2 hrs 22 min and 4 hrs 22 min respectively, after the initial exposure, the higher T_{max} (lower-volatility) mode is visible and dominates the thermogram.

Atmos. Chem. Phys. Discuss., https://doi.org/10.5194/acp-2019-271
Manuscript under review for journal Atmos. Chem. Phys.
Discussion started: 8 April 2019

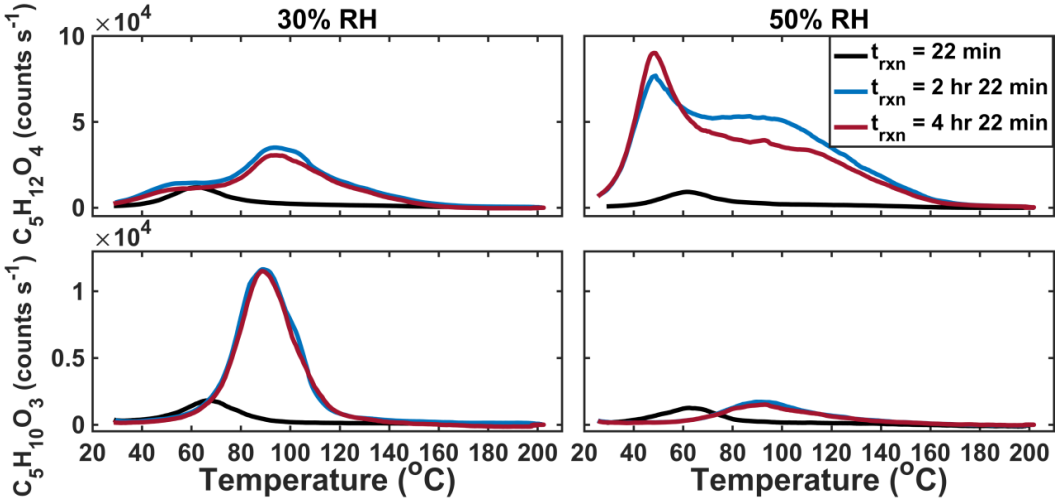

Figure 6. Sequential desorptions of $C_5H_{12}O_4$ (top) and $C_5H_{10}O_3$ (bottom) during batch mode experiments at 30% RH (right) and 50% RH (left).

In the 50% RH batch experiment, the lower T_{max} (higher-volatility) mode of the $C_5H_{12}O_4$ thermogram also dominates in the first desorption, but in contrast to the experiment at 30% RH, this lower T_{max} mode continues to grow and is the dominant portion of the thermogram for all desorptions. While the higher T_{max} mode is observed after the 1st desorption, it is much broader and has an ambiguous peak, unlike at 30% RH. In the 30% and 50% RH experiments, both modes of the thermogram are observed by the 2nd desorption 2.5 hours after IEPOX uptake starts, but the relative abundance and shape of the two modes differ with RH. The thermogram shape also changes as a function of time since IEPOX injection in the steady state experiments, although due to the range in aerosol ages present within the chamber at a given time during steady-state experiments, it is more straightforward to define this feature as a function of time in batch mode measurements. The corresponding thermograms of $C_5H_{10}O_3$ in each of the two batch mode experiments are shown in Figure 6, bottom. Most obvious is that the amount of $C_5H_{10}O_3$ desorbing, relative to the 2-methyltetrol, is highest in the 30% RH experiment, when sulfate and hydronium ion concentrations are highest. Further work could be done to understand the evolution of IEPOX SOA components as a function of time, but a fairly stable set of products and volatility are reached within a few hours.

Along with the shape, the T_{max} of the $C_5H_{10}O_3$ and each mode of the $C_5H_{12}O_4$ vary slightly in time, the two of which are likely related. It has been shown previously that when the IEPOX-derived organosulfate ($C_5H_{12}SO_7$) is deposited on and desorbed from the FIGAERO filter, it decomposes into both $C_5H_{12}O_4$ and $C_5H_{10}O_3$. The corresponding T_{max} of both are co-located and highly dependent on acidity, with higher acidity leading to lower T_{max}'s (Lopez-Hilfiker et al., 2016). This dependence on the inorganic aerosol components, present in much larger excess in these experiments than our previous FIGAERO experiments, could be the cause of the shifts of the lower T_{max} modes. Alternatively, the shift could be due to the increasing complexity of the SOA as it evolves in time leading to different interactions between particle components which affects volatility.

From these observations we can draw two conclusions regarding the mechanisms that give rise to the dominant components of IEPOX SOA, illustrated in Figure 7. First, the low T_{max},

Atmos. Chem. Phys. Discuss., https://doi.org/10.5194/acp-2019-271
Manuscript under review for journal Atmos. Chem. Phys.
Discussion started: 8 April 2019

Atmospheric Chemistry and Physics Discussions

semi-volatile $C_5H_{12}O_4$ exists in the aerosol from the first desorption and thus is likely formed promptly from IEPOX uptake, consistent with the formation of 2-methyltetrol via nucleophilic attack by water of the protonated epoxide ring (see Figure 7). That this semi-volatile mode is more prominent in the higher RH experiment, i.e. higher liquid water content and therefore higher H_2O-nucleophile content relative to sulfate, further supports this interpretation. Additionally, the higher liquid water content supports a greater amount of 2-methyltetrol remaining partitioned in the aerosol via Henry's Law, consistent with offline filter analysis (Riva et al., 2016). Second, the higher T_{max} (lower volatility) modes are mostly produced more slowly over time, indicating a second or higher generation product of IEPOX uptake, as these modes are mainly observed 2.5 hours after IEPOX uptake has largely ended. Thus, if the higher T_{max} modes are from the thermal decomposition of an organosulfate product, as suggested by Lopez-Hilfiker et al. (2016) and as Cui et al. (2018) demonstrate, our experiments suggest it is unlikely to form solely from nucleophilic addition of (bi-)sulfate to protonated IEPOX, as that reaction should occur concurrently with 2-methyltetrol formation.

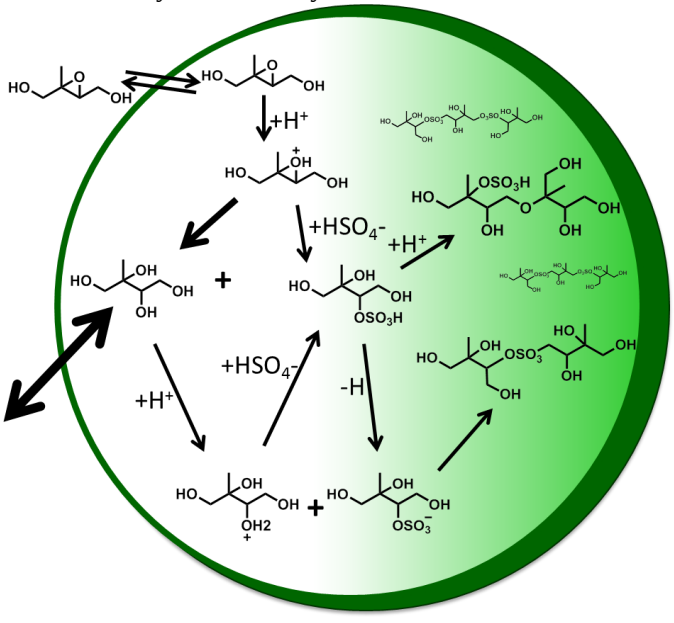

Figure 7. Schematic of IEPOX reactive uptake and particle-phase processes. White region denotes semi volatile species that actively partition between the gas- and particle-phases, light green denotes species that are of lower volatility, and dark green outline denotes a coating.

Another possible mechanism of organosulfate formation, as well as sulfate ester oligomers, is via S_N2 reactions where one of the 2-methyltetrol –OH groups is protonated to make H_2O the leaving group while bisulfate, sulfate, or an organosulfate is the substituting group (Figure 7). At 30% RH, the particle acidity is higher due to less dilution of the sulfate, which would result in higher organosulfate concentrations and acid catalyzed accretion chemistry (Jang et al., 2002), consistent with the observation of a more prominent higher T_{max} (lower volatility) mode compared to the 50% RH experiment. The broader higher T_{max} mode at 50% RH indicates that there is likely an array of compounds breaking apart to give rise to this specific composition, consistent with a greater variety of oligomerization reactions occurring due to the dilution of

Atmos. Chem. Phys. Discuss., https://doi.org/10.5194/acp-2019-271
Manuscript under review for journal Atmos. Chem. Phys.
Discussion started: 8 April 2019

Atmospheric Chemistry and Physics Discussions

sulfate and higher 2-methyltetrol concentrations. Previous work has identified several non-sulfur containing polyol species, both monomers and oligomers, in IEPOX SOA (Lin et al., 2012; Surratt et al., 2010).

Summary & Atmospheric Implications

To place our findings into context, we present results from a simple conceptual model simulating IEPOX (initially 2 ppb) reactive uptake to form the corresponding 2-methyltetrol and organosulfate at yields of 90 and 10%, respectively, with an uptake coefficient of 0.05 based on Gaston et al. (2014), and an atmospherically relevant total surface area (2.5×10^{-6} cm^2 cm^{-3}) and volume (1.6×10^{-11} cm^3 cm^{-3}). We also include a loss of gas-phase 2-methyltetrol and IEPOX due to reaction with OH (Atkinson, 1987). The processes in the model are simplified from the reaction scheme discussed above, i.e. it does not include particle-phase processes, but its purpose is to capture the salient factors that control the reactive uptake and partitioning. The chosen branching between 2-methyltetrol and organosulfate yields from IEPOX reactive uptake to aerosol is somewhat arbitrary and only to illustrate the behavior of the system. The Henry's Law constant found via COSMOtherm for the 2-methyltetrol is used to simulate gas-particle partitioning of the 2-methyltetrol, while the organosulfate is a proxy for all low volatility products, including the promptly formed organosulfates, sulfate esters from further accretion, and polyol oligomers.

The simulated loss of IEPOX and formation of IEPOX SOA are shown in Figure 8. IEPOX is almost completely consumed after 1 hour of reaction, corresponding to rapid formation of SOA. The composition of the aerosol changes significantly as a function of time. Initially, the SOA is composed primarily of 2-methyltetrol. However, despite the relatively high Henry's law constant, much of the 2-methyltetrol evaporates into the gas-phase to maintain equilibrium with the gas-phase 2-methyltetrol which is subjected to loss by gas-phase bimolecular reactions with the hydroxyl radical (OH). This behavior supports our findings herein that on a typical aerosol lifetime, the dominant IEPOX reactive uptake product, 2-methyltetrol, will be a small component of IEPOX SOA, and organosulfates and other low volatility material, including oligomers of 2-methyltetrol, will dominate, albeit at a smaller overall SOA yield (Figure 8) per IEPOX reacting on aerosol.

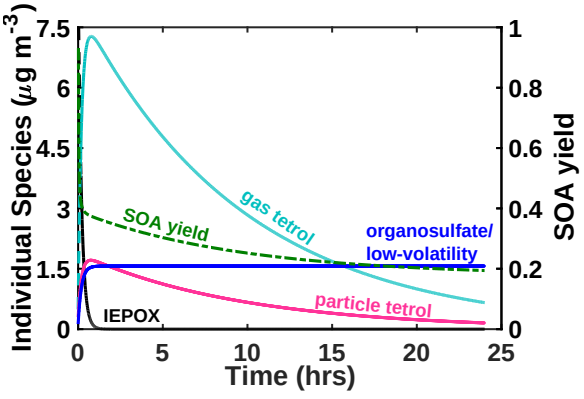

Figure 8. Model results for the major gas- and particle-phase species of IEPOX reactive uptake for typical atmospheric aerosol and typical IEPOX mixing ratios.

Fundamental chamber studies of IEPOX reactive uptake to aqueous acidic seed were performed and we find that the resulting molecular composition and volatility of the formed SOA confirm that the vast majority of IEPOX SOA in the atmosphere is of very low volatility, in the form of organosulfates and polyol oligomers. We show that the major product expected from IEPOX reactive uptake in acidic aqueous solutions, the 2-methyltetrol, is semi-volatile and likely will partition out of the aerosol and thus contribute relatively little to IEPOX SOA mass under atmospheric conditions. We further confirm that C_5-alkene triols and/or 3-MeTHF-3,4-diols are not components of IEPOX SOA but rather artifacts of thermal decomposition during analytical workup, and should not be included as products in mechanistic models of IEPOX SOA formation and evolution. Finally, we provide evidence that a portion of the low volatility IEPOX SOA is composed of oligomers formed in part from slower particle-phase accretion chemistry, likely involving the first generation organosulfates and possibly also the 2 methyl-tetrol, though we can't distinguish between these possible combinations. The distribution of products and formation timescales depend upon aerosol water, sulfate, and hydronium ion activities, and thus ultimately on ambient RH and particle alkalinity sources.

These findings help to resolve inconsistencies in the descriptions of IEPOX SOA formation from gas-phase IEPOX reactive uptake. The low SOA yield per reactive uptake of IEPOX on aqueous acidic seed can be explained as 2-methyltetrol, the dominant product, being semi-volatile and largely partitioning out of the particle-phase especially in a system with gas-phase oxidation or in chambers with vapor-wall loss. Measured reactive uptake probabilities of IEPOX (γ_{IEPOX}) on aqueous acidic seed are an order of magnitude or more higher than often used in models (Eddingsaas et al., 2010; Gaston et al., 2014; Marais et al., 2016; Pye et al., 2013). Partly this discrepancy reflects a lower SOA yield per IEPOX lost than accounted for in models, for which we provide an explanation, and also a role for organic coatings that likely exist in the atmosphere which slow reactive uptake relative to pure aqueous acidic seed (Gaston et al., 2014; Zhang et al., 2018).

These aspects likely have some cancelation of errors, but could lead to errors in models of IEPOX abundance and the IEPOX SOA production rate, and thus their corresponding spatial variability. For example, in regions with relatively fresh, uncoated aqueous acidic particles, models using a low reaction probability would underestimate the IEPOX loss rate from the gas-phase, sustaining IEPOX SOA formation over a larger area than in reality. A model that ignored the role of organic coatings and 2-methyltetrol evaporation would potentially overestimate IEPOX SOA formation on regional scales. Models that treat products of IEPOX reactive uptake in a volatility basis set would need to utilize the volatility inferred from the thermograms herein, or thermal denuder measurements, rather than that inferred from commonly reported IEPOX SOA tracers that utilize high-temperature analytical methods like GC/MS. Finally, without accounting for slower accretion chemistry involving organosulfates and polyols, IEPOX SOA predicted from a treatment of first generation products alone could be underestimated.

Author Contributions

E.L.D. analyzed FIGAERO data; E.L.D., J.A.T., and S.S. conducted modeling; and E.L.D. and J.A.T. wrote the manuscript. J.E.S. and J.A.T designed the chamber experiments. N.H., V-T. S., G.H., and T.K made COSMOtherm predictions. All other coauthors participated in data collection, experiment operations, and manuscript discussions.

Acknowledgements

This work was supported by the U.S. Department of Energy ASR grants DE-SC0011791 and DE-SC0018221. E.L.D was supported by the National Science Foundation Graduate Research Fellowship under Grant No. DGE-1256082. PNNL authors were supported by the U.S. Department of Energy, Office of Biological and Environmental Research, as part of the ASR program. Pacific Northwest National Laboratory is operated for DOE by Battelle Memorial Institute under contract DE-AC05-76RL01830. UC Davis authors were supported by NSF grant ATM-1151062. We thank A. Gold and Z. Zhang for synthesizing the *trans*-β-IEPOX, 2-methyltetrol, and 3-MeTHG-3,4-diol standards used in this work.

References

Atkinson, R.: A Structure-Activity Relationship for the Estimation of Rate Constants for the Gas-Phase Reactions of OH Radicals with Organic-Compounds International Journal of Chemical Kinetics, 19, 799-828, doi: 10.1002/kin.550190903, 1987.

Bates, K. H., Crounse, J. D., St Clair, J. M., Bennett, N. B., Nguyen, T. B., Seinfeld, J. H., Stoltz, B. M., and Wennberg, P. O.: Gas phase production and loss of isoprene epoxydiols, The Journal of Physical Chemistry A, 118, 1237-1246, doi: 10.1021/jp4107958, 2014.

Bondy, A. L., Craig, R. L., Zhang, Z., Gold, A., Surratt, J. D., and Ault, A. P.: Isoprene-Derived Organosulfates: Vibrational Mode Analysis by Raman Spectroscopy, Acidity-Dependent Spectral Modes, and Observation in Individual Atmospheric Particles, The Journal of Physical Chemistry A, 122, 303-315, doi: 10.1021/acs.jpca.7b10587, 2018.

Compernolle, S., Ceulemans, K., and Muller, J. F.: EVAPORATION: a new vapour pressure estimation method for organic molecules including non-additivity and intramolecular interactions, Atmos. Chem. Phys., 11, 9431-9450, doi: 10.5194/acp-11-9431-2011, 2011.

Cui, T., Zeng, Z., dos Santos, E. O., Zhang, Z., Chen, Y., Zhang, Y., Rose, C. A., Budisulistiorini, S. H., Collins, L. B., Bodnar, W. M., de Souza, R. A. F., Martin, S. T., Machado, C. M. D., Turpin, B. J., Gold, A., Ault, A. P., and Surratt, J. D.: Development of a hydrophilic interaction liquid chromatography (HILIC) method for the chemical characterization of water-soluble isoprene epoxydiol (IEPOX)-derived secondary organic aerosol, Environmental Science: Processes & Impacts, doi: 10.1039/c8em00308d, 2018.

D'Ambro, E. L., Lee, B. H., Liu, J., Shilling, J. E., Gaston, C. J., Lopez-Hilfiker, F. D., Schobesberger, S., Zaveri, R. A., Mohr, C., Lutz, A., Zhang, Z., Gold, A., Surratt, J. D., Rivera-Rios, J. C., Keutsch, F. N., and Thornton, J. A.: Molecular composition and volatility of isoprene photochemical oxidation secondary organic aerosol under low- and high-NOx conditions, Atmos. Chem. Phys., 17, 159-174, doi: 10.5194/acp-17-159-2017, 2017a.

D'Ambro, E. L., Moller, K. H., Lopez-Hilfiker, F. D., Schobesberger, S., Liu, J. M., Shilling, J. E., Lee, B., Kjaergaard, H. G., and Thornton, J. A.: Isomerization of Second-Generation Isoprene Peroxy Radicals: Epoxide Formation and Implications for Secondary Organic Aerosol Yields, Environmental science & technology, 51, 4978-4987, doi: 10.1021/acs.est.7b00460, 2017b.

D'Ambro, E. L., Schobesberger, S., Zaveri, R. A., Shilling, J. E., Lee, B. H., Lopez-Hilfiker, F. D., Mohr, C., and Thornton, J. A.: Isothermal Evaporation of α-Pinene Ozonolysis SOA: Volatility, Phase State, and Oligomeric Composition, ACS Earth and Space Chemistry, doi: 10.1021/acsearthspacechem.8b00084, 2018.

Eddingsaas, N. C., VanderVelde, D. G., and Wennberg, P. O.: Kinetics and products of the acid-catalyzed ring-opening of atmospherically relevant butyl epoxy alcohols, J. Phys. Chem. A, 114, 8106-8113, doi: 10.1021/jp103907c, 2010.

Gaston, C. J., Riedel, T. P., Zhang, Z. F., Gold, A., Surratt, J. D., and Thornton, J. A.: Reactive uptake of an isoprene-derived epoxydiol to submicron aerosol particles, Environ. Sci. Technol., 48, 11178-11186, doi: 10.1021/es5034266, 2014.

Guenther, A. B., Jiang, X., Heald, C. L., Sakulyanontvittaya, T., Duhl, T., Emmons, L. K., and Wang, X.: The model of emissions of gases and aerosols from nature version 2.1 (MEGAN2.1): an extended and updated framework for modeling biogenic emissions, Geosci. Model Dev., 5, 1471-1492, doi: 10.5194/gmd-5-1471-2012, 2012.

Hallquist, M., Wenger, J. C., Baltensperger, U., Rudich, Y., Simpson, D., Claeys, M., Dommen, J., Donahue, N. M., George, C., Goldstein, A. H., Hamilton, J. F., Herrmann, H., Hoffmann, T., Iinuma, Y., Jang, M., Jenkin, M. E., Jimenez, J. L., Kiendler-Scharr, A., Maenhaut, W., McFiggans, G., Mentel, T. F., Monod, A., Prevot, A. S. H., Seinfeld, J. H., Surratt, J. D., Szmigielski, R., and Wildt, J.: The formation, properties and impact of secondary organic aerosol: current and emerging issues, Atmospheric Chemistry and Physics, 9, 5155-5236, 2009.

628 Jang, M. S., Czoschke, N. M., Lee, S., and Kamens, R. M.: Heterogeneous atmospheric aerosol
629 production by acid-catalyzed particle-phase reactions, Science, 298, 814-817, doi:
630 10.1126/science.1075798, 2002.
631 Kurtén, T., Hyttinen, N., D'Ambro, E. L., Thornton, J., and Prisle, N. L.: Estimating the saturation vapor
632 pressures of isoprene oxidation products C5H12O6 and C5H10O6 using COSMO-RS, Atmos.
633 Chem. Phys., 18, 17589-17600, doi: 10.5194/acp-18-17589-2018, 2018.
634 Lee, B. H., Lopez-Hilfiker, F. D., Mohr, C., Kurten, T., Worsnop, D. R., and Thornton, J. A.: An iodide-
635 adduct high-resolution time-of-flight chemical-ionization mass spectrometer: application to
636 atmospheric inorganic and organic compounds, Environ. Sci. Technol., 48, 6309-6317, doi:
637 10.1021/es500362a, 2014.
638 Lin, Y. H., Zhang, Z. F., Docherty, K. S., Zhang, H. F., Budisulistiorini, S. H., Rubitschun, C. L., Shaw,
639 S. L., Knipping, E. M., Edgerton, E. S., Kleindienst, T. E., Gold, A., and Surratt, J. D.: Isoprene
640 epoxydiols as precursors to secondary organic aerosol formation: Acid-catalyzed reactive uptake
641 studies with authentic compounds, Environ. Sci. Technol., 46, 250-258, doi: 10.1021/es202554c,
642 2012.
643 Lin, Y. H., Budisulistiorini, H., Chu, K., Siejack, R. A., Zhang, H. F., Riva, M., Zhang, Z. F., Gold, A.,
644 Kautzman, K. E., and Surratt, J. D.: Light-absorbing oligomer formation in secondary organic
645 aerosol from reactive uptake of isoprene epoxydiols, Environ. Sci. Technol., 48, 12012-12021,
646 doi: 10.1021/es503142b, 2014.
647 Liu, J. M., D'Ambro, E. L., Lee, B. H., Lopez-Hilfiker, F. D., Zaveri, R. A., Rivera-Rios, J. C., Keutsch,
648 F. N., Iyer, S., Kurten, T., Zhang, Z. F., Gold, A., Surratt, J. D., Shilling, J. E., and Thornton, J.
649 A.: Efficient isoprene secondary organic aerosol formation from a non-IEPOX pathway, Environ.
650 Sci. Technol., 50, 9872-9880, doi: 10.1021/acs.est.6b01872, 2016.
651 Liu, S., Shilling, J. E., Song, C., Hiranuma, N., Zaveri, R. A., and Russell, L. M.: Hydrolysis of
652 organonitrate functional groups in aerosol particles, Aerosol Sci. Technol., 46, 1359-1369, doi:
653 10.1080/02786826.2012.716175, 2012.
654 Lopez-Hilfiker, F. D., Mohr, C., Ehn, M., Rubach, F., Kleist, E., Wildt, J., Mentel, T. F., Lutz, A.,
655 Hallquist, M., Worsnop, D., and Thornton, J. A.: A novel method for online analysis of gas and
656 particle composition: description and evaluation of a Filter Inlet for Gases and AEROsols
657 (FIGAERO), Atmos. Meas. Tech., 7, 983-1001, doi: 10.5194/amt-7-983-2014, 2014.
658 Lopez-Hilfiker, F. D., Mohr, C., D'Ambro, E. L., Lutz, A., Riedel, T. P., Gaston, C. J., Iyer, S., Zhang, Z.,
659 Gold, A., Surratt, J. D., Lee, B. H., Kurten, T., Hu, W. W., Jimenez, J., Hallquist, M., and
660 Thornton, J. A.: Molecular composition and volatility of organic aerosol in the southeastern US:
661 Implications for IEPOX derived SOA, Environ. Sci. Technol., 50, 2200-2209, doi:
662 10.1021/acs.est.5b04769, 2016.
663 Marais, E. A., Jacob, D. J., Jimenez, J. L., Campuzano-Jost, P., Day, D. A., Hu, W., Krechmer, J., Zhu,
664 L., Kim, P. S., Miller, C. C., Fisher, J. A., Travis, K., Yu, K., Hanisco, T. F., Wolfe, G. M.,
665 Arkinson, H. L., Pye, H. O. T., Froyd, K. D., Liao, J., and McNeill, V. F.: Aqueous-phase
666 mechanism for secondary organic aerosol formation from isoprene: application to the southeast
667 United States and co-benefit of SO2 emission controls, Atmos. Chem. Phys., 16, 1603-1618, doi:
668 10.5194/acp-16-1603-2016, 2016.
669 Paulot, F., Crounse, J. D., Kjaergaard, H. G., Kurten, A., St Clair, J. M., Seinfeld, J. H., and Wennberg, P.
670 O.: Unexpected epoxide formation in the gas-phase photooxidation of isoprene, Science, 325,
671 730-733, doi: 10.1126/science.1172910, 2009.
672 Pye, H. O. T., Pinder, R. W., Piletic, I. R., Xie, Y., Capps, S. L., Lin, Y. H., Surratt, J. D., Zhang, Z. F.,
673 Gold, A., Luecken, D. J., Hutzell, W. T., Jaoui, M., Offenberg, J. H., Kleindienst, T. E.,
674 Lewandowski, M., and Edney, E. O.: Epoxide pathways improve model predictions of isoprene
675 markers and reveal key role of acidity in aerosol formation, Environmental science & technology,
676 47, 11056-11064, doi: 10.1021/es402106h, 2013.
677 Riedel, T. P., Lin, Y. H., Budisulistiorini, H., Gaston, C. J., Thornton, J. A., Zhang, Z. F., Vizuete, W.,
678 Gold, A., and Surrattt, J. D.: Heterogeneous reactions of isoprene-derived epoxides: reaction

probabilities and molar secondary organic aerosol yield estimates, Environ. Sci. Technol. Lett., 2, 38-42, doi: 10.1021/ez500406f, 2015.

Riva, M., Budisulistiorini, S. H., Chen, Y. Z., Zhang, Z. F., D'Ambro, E. L., Zhang, X., Gold, A., Turpin, B. J., Thornton, J. A., Canagaratna, M. R., and Surratt, J. D.: Chemical characterization of secondary organic aerosol from oxidation of isoprene hydroxyhydroperoxides, Environ. Sci. Technol., 50, 9889-9899, doi: 10.1021/acs.est.6b02511, 2016.

Schobesberger, S., D'Ambro, E. L., Lopez-Hilfiker, F. D., Mohr, C., and Thornton, J. A.: A model framework to retrieve thermodynamic and kinetic properties of organic aerosol from composition-resolved thermal desorption measurements, Atmos. Chem. Phys., 18, 14757-14785, doi: 10.5194/acp-18-14757-2018, 2018.

St Clair, J. M., Rivera-Rios, J. C., Crounse, J. D., Knap, H. C., Bates, K. H., Teng, A. P., Jørgensen, S., Kjaergaard, H. G., Keutsch, F. N., and Wennberg, P. O.: Kinetics and products of the reaction of the first-generation isoprene hydroxy hydroperoxide (ISOPOOH) with OH, J. Phys. Chem. A, 120, 1441-1451, doi: 10.1021/acs.jpca.5b06532, 2016.

Surratt, J. D., Murphy, S. M., Kroll, J. H., Ng, N. L., Hildebrandt, L., Sorooshian, A., Szmigielski, R., Vermeylen, R., Maenhaut, W., Claeys, M., Flagan, R. C., and Seinfeld, J. H.: Chemical composition of secondary organic aerosol formed from the photooxidation of isoprene, J. Phys. Chem. A, 110, 9665-9690, doi: 10.1021/jp061734m, 2006.

Surratt, J. D., Kroll, J. H., Kleindienst, T. E., Edney, E. O., Claeys, M., Sorooshian, A., Ng, N. L., Offenberg, J. H., Lewandowski, M., Jaoui, M., Flagan, R. C., and Seinfeld, J. H.: Evidence for organosulfates in secondary organic aerosol, Environ. Sci. Technol., 41, 517-527, doi: 10.1021/es062081q, 2007a.

Surratt, J. D., Lewandowski, M., Offenberg, J. H., Jaoui, M., Kleindienst, T. E., Edney, E. O., and Seinfeld, J. H.: Effect of acidity on secondary organic aerosol formation from isoprene, Environ. Sci. Technol., 41, 5363-5369, doi: 10.1021/es0704176, 2007b.

Surratt, J. D., Chan, A. W. H., Eddingsaas, N. C., Chan, M. N., Loza, C. L., Kwan, A. J., Hersey, S. P., Flagan, R. C., Wennberg, P. O., and Seinfeld, J. H.: Reactive intermediates revealed in secondary organic aerosol formation from isoprene, Proc. Natl. Acad. Sci. U. S. A., 107, 6640-6645, doi: 10.1073/pnas.0911114107, 2010.

Wang, W., Kourtchev, I., Graham, B., Cafmeyer, J., Maenhaut, W., and Claeys, M.: Characterization of oxygenated derivatives of isoprene related to 2-methyltetrols in Amazonian aerosols using trimethylsilylation and gas chromatography/ion trap mass spectrometry, Rapid Commun. Mass Spectrom., 19, 1343-1351, doi: 10.1002/rcm.1940, 2005.

Watanabe, A. C., Stropoli, S. J., and Elrod, M. J.: Assessing the Potential Mechanisms of Isomerization Reactions of Isoprene Epoxydiols on Secondary Organic Aerosol, Environmental science & technology, 52, 8346-8354, doi: 10.1021/acs.est.8b01780, 2018.

Waxman, E. M., Elm, J., Kurtén, T., Mikkelsen, K. V., Ziemann, P. J., and Volkamer, R.: Glyoxal and Methylglyoxal Setschenow Salting Constants in Sulfate, Nitrate, and Chloride Solutions: Measurements and Gibbs Energies, Environmental science & technology, 49, 11500-11508, doi: 10.1021/acs.est.5b02782, 2015.

Wexler, A. S., and Clegg, S. L.: Atmospheric aerosol models for systems including the ions H+, NH4+, Na+, SO42-, NO3-,Cl-, Br-, and H2O, J. Geophys. Res.-Atmos., 107, doi: 10.1029/2001jd000451, 2002.

Zhang, Y., Chen, Y., Lambe, A. T., Olson, N. E., Lei, Z., Craig, R. L., Zhang, Z., Gold, A., Onasch, T. B., Jayne, J. T., Worsnop, D. R., Gaston, C. J., Thornton, J. A., Vizuete, W., Ault, A. P., and Surratt, J. D.: Effect of the Aerosol-Phase State on Secondary Organic Aerosol Formation from the Reactive Uptake of Isoprene-Derived Epoxydiols (IEPOX), Environ. Sci. Technol. Lett., 5, 167-174, doi: 10.1021/acs.estlett.8b00044, 2018.

Zhang, Z., Lin, Y. H., Zhang, H., Surratt, J. D., Ball, L. M., and Gold, A.: Technical Note: Synthesis of isoprene atmospheric oxidation products: isomeric epoxydiols and the rearrangement products

729 cis- and trans-3-methyl-3,4-dihydroxytetrahydrofuran, Atmos. Chem. Phys., 12,
730 8529-8535, doi: 10.5194/acp-12-8529-2012, 2012.

731

732